E-Fi: Evasive Wi-Fi Measures for Surviving LTE within 5GHz Unlicensed Band

Carlos Bocanegra, *Student Member, IEEE,* Takai Eddine Kennouche, *Member, IEEE,*
Zhengnan Li, *Student Member, IEEE,* Lorenzo Favalli, *Member, IEEE,* Marco Di Felice,
and Kaushik Chowdhury, *Senior Member, IEEE*

Abstract—The growing spectrum crunch has motivated exploratory efforts in the use of LTE in the 5GHz bands for downlink traffic. However, this paradigm raises concerns of fair sharing of the spectrum and the adverse impact of scheduled LTE frames on Wi-Fi Packet Success Rates (PSR). To address this issue, we propose E-Fi, an interference-evasion mechanism that allows Wi-Fi devices to survive LTE transmissions without any cooperation between these two different standards. Different from existing approaches, we argue that the simple use of *Almost Blank Subframes* (ABS) within the LTE standard offering short channel access windows overestimates opportunities for Wi-Fi. The pilots embedded in the ABS not only interfere with Wi-Fi but also adversely impact the carrier sensing function. E-Fi mitigates this problem through a two-fold approach. It uses a combination of (i) Wi-Fi Direct with packet relaying and (ii) classical distributed coordination function to reach distant nodes. Second, it ensures load balancing for both Wi-Fi uplink and downlink traffic with high PSR by creating node-groups based with dedicated contention-based medium access intervals. Our approach is validated by comprehensive simulation and experimental results that indicate significantly higher throughput in E-Fi compared to classical Wi-Fi.

Index Terms—Coexistence, unlicensed band, LTE, Wi-Fi, optimal scheduling, matching, Hungarian algorithm, Almost Blank Subframes (ABS), Packet Error Rate (PER), Cell specific Reference Signals (CRS), further enhanced Inter-Cell Interference Coordination (feICIC).

---✦---

1 INTRODUCTION

CELLULAR traffic has increased 4000 times over the last ten years, propelled by the growing adoption of smartphones nearing 50% of the electronic device market [1]. Furthermore, emerging areas like the Internet of Things predict billions of connected sensors worldwide within next few years, which will further stress existing communication infrastructures. One solution to this problem is the proposed LTE Unlicensed (LTE-U) paradigm that uses the 5 GHz band for both enterprise-driven LTE and Wi-Fi networks by assimilating spectrum from the unlicensed bands. However, the strict time-bound frame transmissions within LTE and its extensive error recovery mechanisms raise concerns on the starvation of Wi-Fi in such shared spectrum use. This paper attempts to address this issue by first demonstrating the limitations of existing standards-specified coexistence techniques and then devising a new approach called Evasive WiFi (E-Fi) that combines Wi-Fi Direct and classical 802.11 distributed coordination function (DCF).

When LTE and Wi-Fi coexist in the same spectrum, LTE is barely impacted, whereas the performance of Wi-Fi drastically degrades to 70-100% packet error rate [2]. LTE Release 10 includes eICIC (enhanced Inter-Cell Interference Coordination) that defines *Almost Blank Subframes* (ABS), which carry neither control nor data information. Primarily aimed for interference management between neighboring

LTE small cells, the reuse of this technique for LTE and Wi-Fi coexistence was introduced in [3]. ABS allows Wi-Fi to gain access to the channel for a short time-frequency window, and by leveraging multiple ABS frames devoid of cellular traffic this window can be extended. There is a fundamental assumption in the research involving ABS scheduling so far: *that Wi-Fi has truly undisturbed channel access during the entirety of the ABS*.

Our studies show that the simplistic assumption of a completely interference-free ABS does not hold true in practice, as the current LTE standards describe mandated and optional reference signals (called pilots henceforth, shown by shaded time-frequency grid units in Figure 1) within the ABS that has significant impact on Wi-Fi. Release 11 includes further eICIC (feICIC), with mechanisms for LTE users to detect and cancel the signals from interfering cells. However, this capability is not present in Wi-Fi receivers. Release 13 describes *Listen Before Talk* (LBT), where LTE is expected to perform carrier sensing and backoff before capturing the unlicensed channel. This proposal, however, has not been adopted in many key markets worldwide, including the U.S. Several prior works have relied on explicit feedback from the Wi-Fi access points (APs) to the LTE base station (BS) for sharing the medium. A differentiating aspect of our work is that the AP and the BS are *unable to explicitly exchange information*; in fact there is no coordination mechanism defined up to the latest, still-evolving LTE Release 14.

• **E-Fi design goals and operational overview:** E-Fi empowers the Wi-Fi AP and its associated nodes to operate alongside LTE transmissions, without dedicated feedback to/from the LTE BS. Instead, it reuses pre-set LTE ABS pat-

- *C. Bocanegra, Z. Li and K. Chowdhury are with Northeastern University, Boston, MA, 02215.*
  E-mail: {bocanegrac, zhengnanlee, krc}@ece.neu.edu
- *T. E. Kennouche and L. Favalli are with University of Pavia, Pavia, 27100.*
  E-mail: {takaieddine.kennouche, lorenzo.favalli}@unipv.it
- *M. Di Felice is with University of Bologna , Bologna, 40126.*
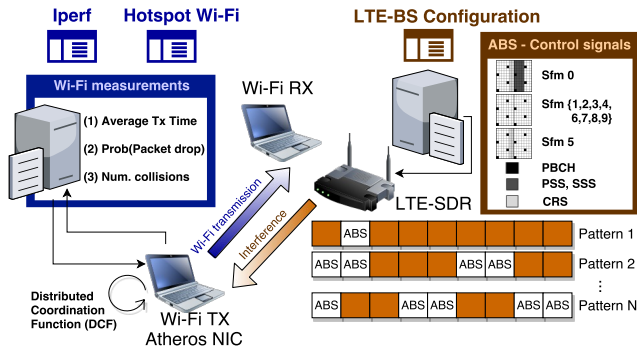 *E-mail: difelice@cs.unibo.it*

Fig. 1. Channel availability experimental set-up using an Atheros NIC, emulating a Wi-Fi device, and srsLTE, running on a Zedboard equipped with the AD-FMCOMMS3, acting as an LTE interferer. The control signals within an ABS Subframe (Sfm) are generated accordingly to the LTE standard and are included in the parent LTE frame [4].
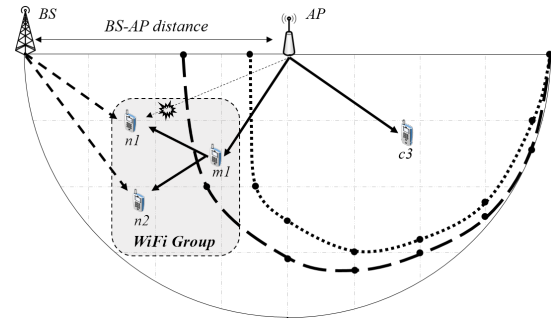

Fig. 2. Example scenario showing impact of different ABS on Wi-Fi packet reception due to the control signals embedded in such frames. Wi-Fi coverage radius is chosen for 90% PSR and 17dBm transmitted power. The dashed and dotted lines define the coverage areas when subframe 1 and 0 are designated ABS, respectively, showing that different subframes allow varying spatial coverage for 90% PSR.

terns to schedule its transmissions. Our solution partitions the Wi-Fi network into self-organizing groups based on the observed PSR, using peer-to-peer communication without a Wi-Fi AP via Wi-Fi Direct [5]. Wi-Fi Direct designates a relay (aka Group Owner), which emulates the Wi-Fi AP, and a Wi-Fi Direct client, which interacts with the Group Owner. In E-Fi, the Group Owner (relaying node) forwards traffic to/from vulnerable nodes that are distant from the AP, but close to the LTE BS. Thus, E-Fi purely looks at the coexistence problem from the Wi-Fi perspective. Recognizing the practical difficulties in providing feedback to the LTE BS, as well avoiding the complexities of solving optimization problems, E-Fi presents an algorithmic framework that enables survival of the Wi-Fi network in uncooperative LTE-U deployments and rogue small-cell installations.

The operating principle of E-Fi rests on three observations: first, not all ABS offer equal transmission opportunities for Wi-Fi. As shown in Figure 1, depending upon where the ABS appears within the parent LTE downlink frame, i.e., its position in one or more of 0-9 subframes, it carries different types of pilot sub-carriers (so-called resource elements in LTE). This in turn requires varying number of committed resource units. For example, ABS 0 has significantly more presence of interfering pilots and offers reduced free channel access compared to others. Second, as shown in the right-hand side of Figure 1, depending upon both the specific ABS frame being considered and the separation between the LTE BS from the Wi-Fi nodes, there is a non-negligible impact on the carrier sensing and deferring process for the latter. Thus, Wi-Fi nodes close to the LTE BS have considerably less chances to transmit a packet [6]. This motivates our approach to schedule Wi-Fi groups into different ABS, hence reducing the number of devices contending for the channel. Third, SINR (and hence BER) can be considerably improved by reducing the transmission distance, which motivates the approach of introducing relay nodes (e.g., m_1 in Figure 2) operating on Wi-Fi Direct. The E-Fi module in the AP carefully assigns uplink and downlink durations (defined on the basis of whether traffic originates at the AP or the nodes) and forms Wi-Fi Direct groups based on reported PSR. Though remote nodes (e.g., n_1 and n_2) now forward their traffic to the AP and vice-versa using

one-hop, this overhead is compensated with high PSR for each link.

• *Contributions:* The main contributions of this work are:

1) We show that the assumptions in [2], [3] that Wi-Fi has undisturbed channel access during the entirety of the ABS is a simplification that has practical impacts on coexistence.

2) Different from most approaches, we design E-Fi under the assumption that the AP and the BS are *unable to explicitly exchange information*. We also do not introduce any changes within the LTE standard.

3) We undertake a methodical study on the impacts on Wi-Fi PSR and carrier sensing mechanism caused by various pilot signals in different ABS configurations through standards-compliant physical layer waveform simulations.

4) We enable self-configuration of Wi-Fi nodes into Wi-Fi Direct groups with forwarding relays using PSR as a selection metric. We then propose a modified Hungarian algorithm with well-defined complexity instead of computationally expensive optimization techniques for the formation of such groups.

5) We formulate an ABS utilization strategy at the AP that partitions contention-based channel access time into distinct intervals, considering individual traffic loads and Wi-Fi Direct relay forwarding overheads.

The rest of the paper is organized as follows: Section II describes the related work. Section III introduces the concept of *safe zones* in E-Fi. Section IV presents E-Fi's spatial relay selection and a group formation strategy. Section V explains the scheduling and channel access mechanisms for single and group node nodes. Section VI validates our approach by means of an integrated MATLAB and NS2 simulation environments. The experimental results are reported in Section VII. Finally, Section VIII concludes the paper.

2 RELATED WORK

LTE-Wi-Fi coexistence strategies can be broadly categorized into spatial multiplexing, frequency multiplexing based on channel selection, time multiplexing using duty cycling, LBT and ABS. Interference management has mainly focused

TABLE 1
Coexistence Scheme Comparison

Category	Coexist scheme	LTE Modification	WiFi Modification	Coordination	Overhead	CRS
Duty Cycle	E-Fi	No	Require PSR			Yes
	E. Almeida [3]	Blank subframe	Dual coex. modes		No	No
	H. Zhang [7]	Spectrum Sensing	Neighbor Discov.	No		
	C. Cano [8]	BS monitors channel			No	N/A
	CSAT [9]	Adaptive DC	No			
	N. Rupasinghe [10]	Q-learning adaptive DC				
	Z. Guan [11]	No	LTE packet sniffing	Yes	LTE	
LBT	T. Tao [12]	Adaptive CW		Yes		N/A
	S. Hajmohammad [13]	Fixed CW	No		No	
	F. Liu [14]	Dual bands		No		
	Y. Li [15]	Adaptive CW	Adaptive CCA th.			

on the downlink due to the asymmetric nature of traffic in LTE, in the order of 8:1 [16]. Duty cycling for coexistence is proposed in [2], [3], [7], [8], [10], [11], [17] whereas, [12], [13], [14], [15] explore other possible coexistence schemes, such as LBT. Additionally, [18], [19], [20] use stochastic geometry in interference and coverage area modeling.

The mutual impact on the performance of LTE and Wi-FI has been studied in [3], [11] taking the average throughput per user as a quality metric. Though [11] proposed a mechanism that is backward compatible with no mutual signaling, Wi-Fi must perform traffic sniffing to predict the ABS pattern. Moreover, the assumption that ABS periods are completely free of all interference limits its application. Two different solutions of Wi-Fi coexistence using ABS and interference avoidance are proposed in [7]. However, the coordinated interference avoidance here relies mostly on cell clustering, and assignment of priority among cells, which requires major modification of current standards. [8] proposed a relatively fair resource allocation method that formulates a convex optimization problem of minimizing LTE-U/Wi-Fi collisions. [21] provides a comprehensive survey of related works. It also presents theoretical models of throughput and overhead for coexisting methods.

A framework that models the channel access of both technologies with LTE adopting the LBT approach is given in [12]. A fixed contention window is set in [13] that limits the performance of LTE in terms of user throughput when collisions occur with Wi-Fi devices. A dual band approach is proposed in [14], where LTE sends its control signals through the licensed band, and offloads data traffic onto the unlicensed band. However, this reduces the spectral efficiency of the system.

Recently, the use of stochastic geometry for characterizing the interference, and modeling the coverage area and throughput in WLAN and LTE systems has gained traction [20]. In [18], a simplistic fluid network model is used to study the ideal coexistence scenario when no multipath and backoff is present. Device-To-Device (D2D) communications for LTE-Wi-Fi coexistence have been proposed in [22], [23] to increase the LTE throughput by offloading some of the messages to Wi-Fi Direct. A spatio-temporal estimation of interference and a load balancing mechanisms are proposed in [24] and [25]. Our approach to use Wi-Fi Direct for relaying purposes is validated in studies like [26], improve-

ments in throughput and energy consumption from D2D are shown ([27] and [28]).

3 WI-FI GROUPS AND RELAYING

In this Section, we show the impact of the pilots within ABS on the Wi-Fi receiver through: (i) physical layer BER and frame detection studies when the AP and the LTE BS transmit standards-complaint waveforms concurrently, and (ii) on the reduction in channel access opportunities for Wi-Fi at the MAC layer. Although ABS do not contain any data or control signals, they may still have multiple embedded pilots (Figure 1): (i) Cell-Specific Reference Signals (CRS), used for power estimation; (ii) Physical Broadcast Channel (PBSCH), used to announce the bandwidth/frequency used by the BS; (iii) Primary Synchronization Channel (PSCH), needed for subframe-level synchronization; and (iv) Secondary Synchronization Channel (SSCH), needed for frame-level synchronization.

3.1 Impact of ABS on 802.11 PHY - Simulation Study

In order to measure the impact on PSR, we create standards-compliant LTE and 802.11n waveforms using MATLAB LTE- and WLAN Systems toolboxes. Here, the LTE BS is deployed as an indoor small cell occupying 20MHz channel in the 5GHz band served by a 802.11n AP. The LTE BS operates in FDD mode with its own link adaptation using the Channel Quality Indicator (CQI) reported by the UE with the default periodicity of 8ms. We select the industry-standard TGn model B with 100ns Delay Spread for the indoor propagation model [29]. The transmission power is set to 17 dBm, following the ITU recommendations in [29] with the noise floor set to -95dBm. The LTE BS is separated by 60m from the Wi-Fi AP, which is also the latter's coverage radius (Figure 2). A transmission is considered successful when the parity check of the signal field returns true and the overall bit error rate (BER) per packet is exactly 0%. Hence, the PSR is the Packet Error Rate (PER) flipped.

Simulation results in Figure 3 show the observed Wi-Fi PSR during ABS 1, plotted as a function of the SINR (that includes LTE interference) and its own received power from the AP. The intersecting horizontal plane indicates the combination of these two measurements that is assured to provide at least 90% PSR (PSR_{Th}). Figure 2 shows
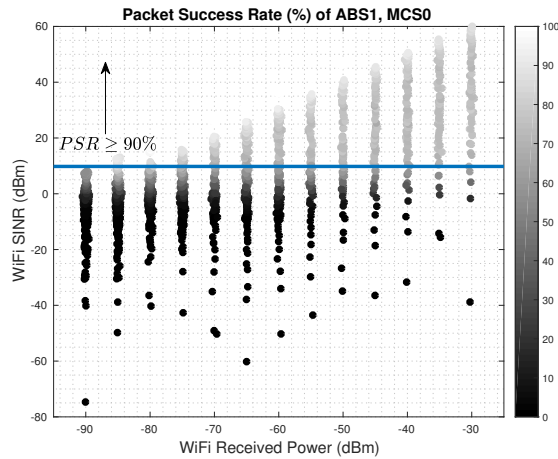
Fig. 3. PSR at the Wi-Fi receiver as a function of the received power and the SINR during concurrent LTE ABS 1 (subframe 1 in LTE frame as ABS) and Wi-Fi transmissions using modulation and coding scheme (MCS) 0 (BPSK and coding rate 1/2).
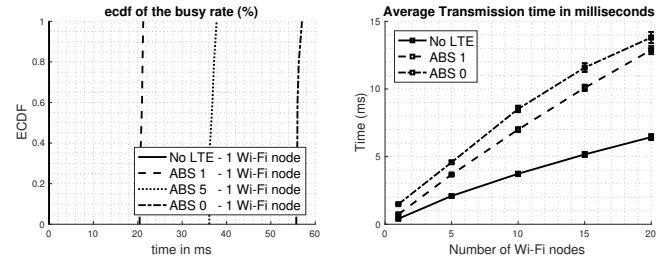

Fig. 4. The CRS embedded within the ABS increase the channel occupancy as shown in the ECDF busy rate (%). As a result, the average time to access the channel and transmit a WiFi packet increases, revealing that the number of CRS impact negatively on the channel accessibility.

two spatial regions of 90% PSR centered around the AP depending upon whether the ABS 0 (inner dotted boundary) or ABS 1 (outer dashed boundary) is used. We call these as *safe zones*. A Wi-Fi device m_j is within the *safe zone* if its PSR is greater than a pre-decided threshold ($PSR_j \geq PSR_{Th}$). In the default implementation of E-Fi, we define the PSR_{Th} to be 90%. Thus, any Wi-Fi node can determine whether it lies within the safe zone by measuring the tuple of SINR and its own received power, even before packet transmissions begin. As we will cover in more detail in further sections, this information is used by E-Fi as a decision criterion to define the three connectivity modes for the Wi-Fi nodes (relay, Wi-Fi Direct node that connects to the AP via the relay, or a regular node that directly connects to the AP).

3.2 Impact of ABS on 802.11 MAC - Experimental Study

The ABS pilots not only affect the Wi-Fi transmission in the downlink, which we quantitatively analyze through the PSR, they also impact the uplink transmissions by reducing channel access opportunities. To characterize this impact, we consider the scenario of a Wi-Fi device continuously attempting to transmit under a continuous presence of ABS type of sub-frames (Figure 1). That is, the LTE received power always exceeds the carrier sensing threshold, leading the Wi-Fi device to backoff.

We modified the srsLTE [30] implementation of the Downlink frames on a USRP B210 series as a way to saturate the channel with LTE frames under different ABS configurations. On the Wi-Fi side, a regular laptop equipped with an Atheros NIC emulates the behavior of an AP attempting to access the channel and operating in saturation mode. We use iperf [31] to generate Downlink traffic from the AP, aiming to fill the MAC queues with outgoing traffic and forcing the driver to always look for transmission opportunities.

The Linux 802.11 configuration API (cfg80211) with the Atheros card and ath9k driver[32] helps in measuring the time the radio is active, and the amount of time the primary channel was sensed busy. There are 4 main functions that are of interest:

- `Ath_get_survey`: This function is called by a user space process and collects the statistics from ath_hw_cycle_counters_update.
- `Ath_hw_cycle_counters_update`: Collects the statistics through some hardware registers (`AR_CCCNT`, `AR_RCCNT`, `AR_RFCNT`, `AR_TFCNT`) that act as an interface between the MAC state machine running on the System on Chip (SoC) and the kernel driver.
- `ath_update_survey_stats`: Converts cycles into seconds according to the clock-rate configured in the system.
- `Ath_tx_complete`: Called whenever a packet is sent out successfully and updates the queue in the Kernel.

The `Ath_get_survey` allows us to extract measurements on the time the channel was sensed busy directly from the driver. The average time to transmit is difficult to obtain, since the drivers do not have access to the stages of the MAC state machine. Thus, there is no reliable way to determine when the backoff counter goes to zero and the packet is transmitted. As a workaround, we employed a debugging mechanism within Linux Kernel called Kprobes [33]. Whenever a message is transmitted to the channel, a flag is set that is detected by ath9k driver. The driver then calls the ath_tx_complete function on the Linux Kernel, clears packets from the queue whenever they are transmitted into the air. Kprobes allows us to track the calls to this function with μs precision [33], thus determining when a packet is transmitted and ultimately allowing for a highly accurate computation of the inter-frame departure time.

The results are shown in Figure 4. The busy rate numbers prove the intuition that the number of control signals has a non-negligible impact on the availability of the channel. Same conclusion can be applied to the time to transmit, where the configuration ABS 0 certainly detriments WiFi's performance. In addition, a high number of devices contending for the channel require greater need of ABS resources. This last observation serves further justifies the grouping procedure in E-Fi, where we reduce the number of contending devices to ensure faster channel access.

Algorithm 1 E-Fi: Group Formation & Resource Dist.

1: LTE presence awareness and ABS detection (Sec. 4.1).
2: PSR Calculation based on P_{RX} and $SINR$ (Sec. 3.1).
3: Pre-categorization into GO_c and WC_c (Sec. 3.1).
4: GO_c discover WC_c and exchange PSR (Sec. 4.2).
5: GO_c follows Eq. (3) to generate candidate set (Sec. 4.3).
6: AP gathers GO_c data to form final groups (Sec. 4.4).
7: AP gathers traffic info and allocates resources (Sec. 5.2).

3.3 Relays for Resilient Transmission during ABS Sub-frames

In this Section, we motivate the key strategy of elevating selected nodes to a relay position to counter the impact of the ABS pilots. These relay nodes forward traffic to and from the AP, connecting remote nodes affected by low PSR. E-Fi requires such relays to become Wi-Fi Direct group owners, and by reducing the link distance in the presence of LTE pilots it improves the collective PSR of the network.

Consider a Wi-Fi AP connected to V nodes in its coverage area and represented by the set $\Omega_{Wi-Fi} = (v_1, v_2, \ldots, v_V)$. An LTE BS serves U user equipments (UEs). The LTE BS can schedule a number of ABS independently of the Wi-Fi, and any such ABS pattern is valid for 40ms. Consider a subset Ω_{SZ} of M nodes that happen to be inside the safe zone ($PSR_j \geq PSR_{Th}$, $\forall j \in \{1, M\}$) and a subset (Ω_{NSZ}) of N nodes that happen to be outside it ($PSR_i < PSR_{Th}$, $\forall i \in \{1, N\}$). Therefore, $V = M + N$. Any device (m_j , $\forall j \in \{1, M\}$) within the safe zone, defined on the basis of PSR, is a potential relay candidate. Those nodes that are outside this range are non-safe zone nodes that attempt to associate with a distinct relay node. All data communication between the relays and such non-safe zone nodes occurs via Wi-Fi Direct within a given ABS. The traffic exchange between the relay and the AP occurs via regular 802.11 in a different ABS.

As we describe in Section 4, E-Fi distributes the available ABS for the two sets of nodes: Set I containing Wi-Fi Direct groups composed of both relays and non-safe zone nodes. Set II containing (i) non-safe zone nodes who are unable to connect to intermediate relays, and (ii) safe zone nodes who do not serve as relays. E-Fi further introduces differential backoff duration to ensure that the remote non-safe zone nodes in Set II (that suffer from lower PSR) get increased transmission opportunities to recover from likely higher errors in Section 5.2. From Figure 5, Set I=$\{m_1, m_2, n_2, n_3, n_4\}$ while Set II=$\{n_1, c_1, c_2\}$.

4 RELAY SELECTION AND DEVICE GROUPING

We formulate the Wi-Fi Direct group formation as a Generalized Assignment Problem (GAP), whose aim is to maximize the number of non-safe zone nodes connected to relays under the objective function of minimizing the average number of transmission in the downlink. Hence, this is the minimization version of GAP or MINGAP [34]). We choose this approach for two reasons- (i) Wi-Fi Direct standard allows a maximum number of 8 connections per group [5] and (ii) high PSR is desired per node in the downlink given the asymmetric flow of traffic. Hence, each group is owned by a relay (m_j, $j \in \{1, M\}$) that serves a set of associated
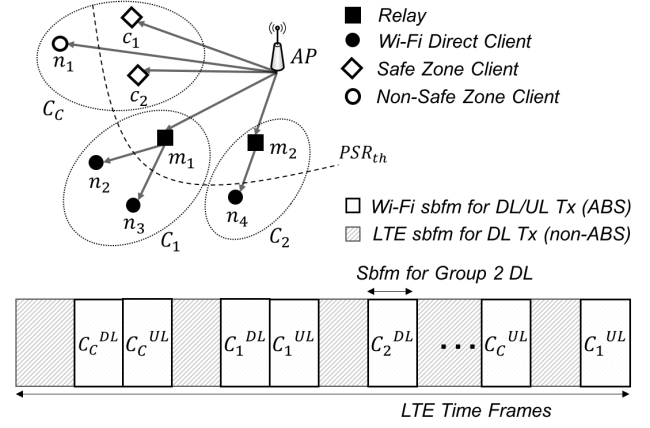

Fig. 5. The safe zone is enclosed by the dashed lines. The nodes are grouped into: $C_c = \{c_1, c_2, n_1\}$; $C_1 = \{m_1, n_2, n_3\}$ and $C_2 = \{m_2, n_4\}$. Group C_1 and C_2 are in Set I while C_c a collection of Set II devices: non-safe zone nodes without relays (n_1) and safe zone nodes who are not relays (c_1 and c_2). At the lower end, sample ABS resource allocation for each group is shown with separate uplink/downlink duration.

non-safe zone nodes (Ψ_j). The cardinality of Ψ_j is denoted by $|\Psi_j|$. All nodes who are not in any relay-owned group are consolidated into Set II and represented by the variable Ψ_C that directly connect to the AP (see Figure 5).

The formal description of the problem is given in Eq. (1), where the objective function is to minimize the number of overall expected transmissions, subject to a maximum number of Wi-Fi device connections K per group and improved PSR for every node in the network compared to direct connection with the AP (Eq. (2)).

$$\min \overline{N_{tx}} = \min \sum_{j \geq 1} \left(\frac{1 + |\Psi_j|}{PSR_{m_j}^{AP}} + \sum_{i \in \Psi_j} \frac{1}{PSR_{n_i}^{m_j}} \right) + \sum_{i \in \Psi_C} \frac{1}{PSR_{n_i}^{AP}} \quad (1)$$

subject to:

$$PSR_{v_i}^* \geq PSR_{v_i} , \ \forall v_i \in \Omega_{Wi-Fi}$$
$$|\Psi_j| \leq K , \ \forall j \in \{1, M\} \quad (2)$$

Here, $PSR_{n_i}^{AP}$, $PSR_{n_i}^{m_j}$ and $PSR_{m_j}^{AP}$ represent the estimated PSR for the direct transmissions by the AP and received at the non-safe zone node, the PSR for transmissions by the relay and received at the node and direct transmissions by the AP and received at the relay, respectively. Other terms are defined earlier in Section 3.3. To ensure that the group formation has bounded complexity, this organization into groups is undertaken centrally at the AP using a modified version of the Hungarian Algorithm [35]. Section 4.4 explains in detail how the constraints of the MINGAP problem are relaxed to reduce it to the Linear Assignment problem (LAP). The proposed algorithm solves the LAP in polynomial time by using PSR collected at the individual nodes and considering all possible non-safe zone node to relay associations from the device discovery phase from Wi-Fi Direct.
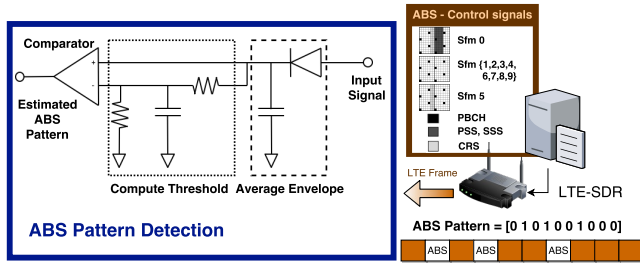
Fig. 6. ABS detection enabled by an envelope detector, which smoothens out the fluctuations, and a comparator, which detects whether the power level exceeds a pre-defined threshold [36]. The LTE interference is generated using a USRP B210 empowered with srsLTE (for further details, see Section 3.2).
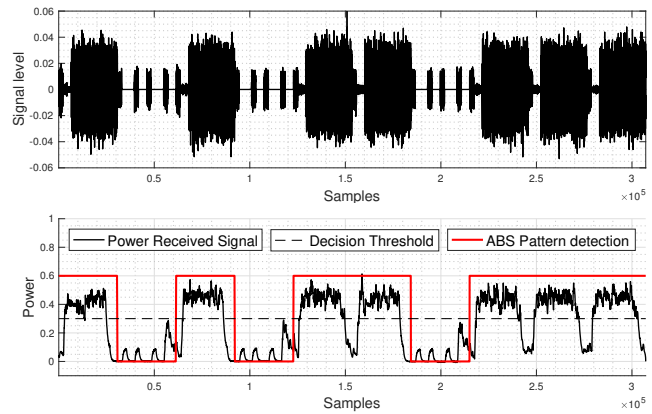

Fig. 7. At the top, the received LTE signal at the entry of the ABS Pattern Detector. The ABS Pattern configured is [0101001000], meaning that the frame embodies 3 ABS (subframes 1, 3 and 6). On the bottom, the signal power detected evolution and the decision whether or not a subframe is ABS or non-ABS based on the threshold.

4.1 Interference Awareness and ABS Pattern detection

A sudden drop in the performance of the Wi-Fi network caused by in-band LTE triggers the initialization of the E-Fi procedure. Consequently, the AP notifies the devices and forces them to defer their transmission and detect the LTE ABS Pattern configured at the BS. Existing methods such as the ones proposed in [37], [38] and [39] use an *RSSI sampler*, available at every Wi-Fi device, to detect and characterize the interference. As for determining the start of the frame, the Wi-Fi devices may employ pattern recognition techniques such as symbol *folding*, which detects periodic signals (i.e. the BCCH in ABS0 and the PSCH/SSCH in the ABS0/5) in noisy environments [40]. Finally, the devices report the measurements to the AP, who announces the start of the discovery phase.

To validate whether these mechanisms can detect ABS over time, we set-up a basic Pattern detector based on the one used in [36] (Figure 6). The detector has two stages. First, a primary stage composed by a diode and a capacitor allows for envelop detection. Second, a combination of resistors and capacitors allows us to compute the threshold by measuring the fluctuations in the signal. For simplicity, the system was configured to provide a threshold equal to $0.5 \cdot (V_{min} + V_{max})$, where V_{min} and V_{max} representing the minimum and maximum voltage, respectively. The LTE frame generation follows the procedure described in detail in Section 3.2, where a USRP B210 sends LTE signals over the air according to the ABS Pattern defined and configured by the srsLTE software.

Figure 7 shows the behavior of the ABS detector. The ABS Pattern configured for this experiments is [0101001000], where subframes 1, 3 and 6 are configured as ABS while the rest carry dummy data. The top figure shows the LTE signal transmitted over the air. In spite of the presence of control signals during ABS, the power level measured at the detector during those is way below the threshold. Thus, allowing the system to clearly differentiate between ABS and non-ABS subframes by comparing it with a predefined and static threshold.

4.2 Device Discovery and PSR Exchange

Once devices are notified, all nodes measure their expected individual PSR (using SINR and received power from AP, see Figure 2) that allows them to self-determine whether they lie in the safe zone. Any node in this zone is a potential relay and assumes the role of a Wi-Fi Direct group leader. It then begins the device discovery process by issuing discovery beacons and logs all non-safe zone nodes that initiate connection requests. Similarly, a given node i that identifies itself to be in the non-safe zone, will send reply beacons containing its ID, the estimated PSR for direct transmissions by the AP, i.e., $PSR_{n_i}^{AP}$, and the estimated PSR for the short-range link between itself and the relay candidate $PSR_{n_i}^{m_j}$. All potential relays also compute their estimated PSR for the AP's transmissions, i.e., $PSR_{m_j}^{AP}$, as this is the metric used to identify which nodes are in safe/non-safe zones.

4.3 Forming Initial Relay Groups

On receiving a set of replies from non-safe zone nodes, the candidate relay m_j determines which neighbor node i would experience improved PSR through a one-hop Wi-Fi Direct-based relaying versus direct AP communication. First, using the measurement of the received power from the non-safe zone nodes, it calculates the new SINR and computes the PSR of the link between itself and the non-safe zone nodes ($PSR_{n_i}^{m_j}$). Second, it checks if the expected number of transmissions through the one-hop communication (w_{ij}^*) is lesser than the direct one to the AP (w_i) for that node, as

$$\overbrace{\frac{1}{PSR_{m_j}^{AP}} + \frac{1}{PSR_{n_i}^{m_j}}}^{w_{ij}{}^*} < \overbrace{\frac{1}{PSR_{n_i}^{AP}}}^{w_i} \qquad (3)$$

The subset Φ_j contains non-safe zone nodes i ($i \in \{1, N\}$) that meet this condition for relay m_j $j \in \{1, M\}$, and hence, benefit from association with it. Each candidate relay node j creates a vector of PSR estimates $\boldsymbol{y}_j$ that includes its own $PSR_{m_j}^{AP}$ as well as the effective PSR w_{ij}^* estimated for the non-safe zone nodes $i \in \Phi_j$ that associate with it as follows

$$\boldsymbol{y}_j = [PSR_{m_j}^{AP} \underbrace{w_{\alpha j}{}^* w_{\beta j}{}^* \dots w_{\gamma j}{}^*}_{\boldsymbol{x}_j}] \quad \forall \alpha, \beta, \gamma \in \Phi_j \qquad (4)$$

TABLE 2
Conditions under which Dummy nodes need to be added to the Bipartite Graph G'. K = maximum number of Wi-Fi Direct nodes, M relays and N non-safe zone nodes.

	$M \cdot N$		$M \cdot K = N$		$M \cdot K > N$	
	$m_j{}'$	AP	$m_j{}'$	AP	$m_j{}'$	AP
$\forall i, j, \ i \neq j, \ s.t.$ $\Phi_i \bigcap \Phi_j = \emptyset$	✓	✓	✗	✗	✓	✗
$\exists i, j; \ i \neq j, \ s.t.$ $\Phi_i \bigcap \Phi_j \neq \emptyset$	✓	✓	✓	✗	✓	✗

This vector is sent to the AP by all the candidate relays. The final group formation is completed at the AP using a modified Hungarian Algorithm (Section 4.4). The individual group membership is then relayed back to the network by the AP.

4.4 Forming Final Groups at the AP

Consider the set of vectors representing PSR measurements reported by all the candidate relay nodes to the AP, i.e., $(\boldsymbol{y}_j, \ \forall j \in \{1, M\})$. It is possible that the same non-safe zone nodes occur in multiple tentative groups formed by the candidate relays. Wi-Fi Direct requires each node to be linked to only one group owner. Hence, the goal of this stage is to (i) finalize the groups such that the nodes connect to one relay only, and (ii) distribute nodes uniformly throughout the groups within the network to maximize the overall PSR. For this purpose, we use a modified Hungarian Algorithm that matches nodes to relays using the PSR vector described above.

4.4.1 Algorithm Description

The AP builds an $N \times (M + 1)$ matrix $\boldsymbol{W}$ containing the measurements vectors $\boldsymbol{x}_j, \ \forall j \in \{1, M\}$ (Eq. (4)), forwarded by N candidate relays (Eq. (5)) as well as the initial PSR values ($w_i, \ \forall i \in \Omega_{Wi-Fi}$). Given that the cardinal of the set Φ_j may vary for different m_j, the AP assigns 0 for the situations where (i) there exists no connection between the relay and the non-safe zone node, or (ii) the one-hop forwarding is not beneficial for that node (i.e., $w_{ij}{}^* = 0 \ \forall i \notin \Phi_j$). Along the same lines, a matrix $\boldsymbol{P}$ is defined as $\boldsymbol{P} = \lim_{n \to \infty}[\boldsymbol{1} - (\boldsymbol{1} - \boldsymbol{W})^n]$. The matrix $\boldsymbol{P}$ contains 1's if the relay communication between m_j and i is beneficial ($w_{ij}{}^* > 0$) and 0's otherwise ($w_{ij}{}^* = 0$).

$$\boldsymbol{W} = \begin{matrix} & \begin{matrix} m_1 & ... & m_M & AP \end{matrix} \\ \begin{matrix} n_1 \\ \vdots \\ n_N \end{matrix} & \begin{pmatrix} w_{11}{}^* & ... & w_{1M}{}^* & \bigg| & w_1 \\ \vdots & \ddots & \vdots & \bigg| & \vdots \\ w_{N1}{}^* & ... & w_{NM}{}^* & \bigg| & w_N \end{pmatrix} \end{matrix} \quad (5)$$

We define the vectors $\boldsymbol{z} = \boldsymbol{P} \cdot \boldsymbol{1}$ and $\boldsymbol{t} = \boldsymbol{1}^t \cdot \boldsymbol{P}$. The former one shows the number of favorable connections for a given node, whereas the latter one shows the number of favorable connections that each relay m_j can offer. In other words, $\boldsymbol{t}$ shows the cardinal of Φ ($t_j = |\Phi_j| \ \forall j \in \{1, M\}$).

We model the network as a Bipartite Graph $G = (C, S, W)$, where the set C contains contains the non-safe zone nodes (Ω_{NSZ}) and the set S contains the candidate relays (Ω_{SZ}) and AP. Recall that the weight of the edge from node n_i ($i \in C$) to relay m_j ($j \in S$) is $w_{ij}{}^*$ and
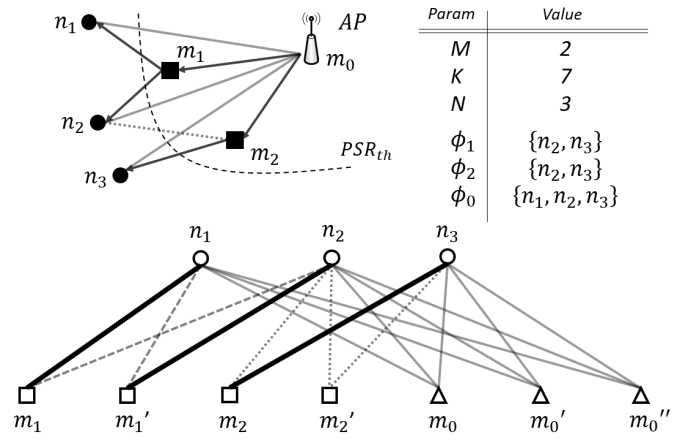

Fig. 8. Modified Bipartite Graph G' given 3 non-safe zone nodes ($N = 3$), 2 candidate relays ($M = 2$) whose number of Wi-Fi Direct connections are limited by the standard ($K = 7$). The final matching is shown in bold, where all the clients (top in G') are connected to exactly one Relay/AP (bottom in G').

that to the AP is w_i. The group formation problem is solved using the Hungarian Algorithm [35], which finds the optimal matching to return the maximum PSR for the entire network. Thus, every node in set C is linked to one node in set S, and after the match, it is removed from the set C. Given that relays can forward traffic to/from more that one node, a modified Bipartite Graph G' is formed by adding dummy relays and APs so that a perfect match can be found. The algorithm terminates when C is an empty set or when no further matches are possible in a given iteration.

Note that all non-safe zone nodes that could not associate with a relay are automatically included in Ψ_C, i.e., the set of all nodes who are not in any relay-owned group. All candidate relay nodes that were not matched with at least one non-safe zone node are also included in Ψ_C. The multiple groups formed through the matching algorithm compose Set I. We show next how the AP distributes the ABS for both these category of nodes based on network loads.

4.4.2 Algorithm Complexity

The Hungarian Algorithm has polynomial complexity given by $O(n^3)$. Although a simplistic solution to form G' would involve adding $(K - 1) \cdot |S|$ dummy relays and $(K - 1) \cdot |S|$ dummy APs to the set S to force the matching, this drastically raises the complexity to $O((2 \cdot K \cdot |S|)^3)$. Instead, E-Fi intelligently adds dummy nodes when needed. Table 2 shows the conditions under which it is necessary to add dummy relays or AP nodes in G' based on the 3-tuple (M, K, N) and the candidate sets Φ with the purpose of minimizing the complexity. Vector $\boldsymbol{t}$ shows the number of nodes that need to be inserted in the modified graph for each node in S. The maximum cardinality of set S is $\boldsymbol{1}^t \cdot \boldsymbol{P} \cdot \boldsymbol{1}$. A simplified scenario is shown in Figure 8 where groups are formed using the modified Bipartite Graph G'. Table 2 shows the need to add two dummy relays ($m_1{}'$ and $m_2{}'$) and dummy APs ($m_0{}'$ and $m_0{}''$). The number of dummy nodes is given by $\boldsymbol{t}$ ($t_1 - 1$ for m_1, $t_2 - 1$ for m_2 and $t_{M+1} - 1$ for m_0).

TABLE 3
Main variables and their definitions

Variable	Definition
M	Total number of Relay Candidates
N	Total number of Nodes outside the S.Z.
m_j	Relay or Relay Candidate j, $\forall j \in \{1, M\}$
n_i	P2P or P2P Candidate j, $\forall i \in \{1, N\}$
Φ_j	P2P Candidate set of m_j
Ψ_j	P2P Nodes attached to m_j, $|\Psi_j| \leq 7$
α	Modified Backoff for DL and UL
w_i , w_j	PSR of Client i and Relay j
$w_{ij}{}^*$, $w_{ji}{}^*$	PSR of n_i through m_j in the DL and UL
λ_{m_j} , λ_{n_i}	Application Load of m_j and n_i
$\eta_j{}^{DL}$, $\eta_j{}^{UL}$	Load Factor of group j in the DL and UL
$|\boldsymbol{A}|_j{}^{DL}$, $|\boldsymbol{A}|_j{}^{UL}$	Number of ABS assigned to group j Tx

5 ABS RESOURCE DISTRIBUTION FOR GROUPS

E-Fi adopts the strategy of fair resource sharing, wherein the AP assigns ABS to individual groups. Further, this resource allocation is done per group and also split between downlink and uplink. The short window of transmission opportunity within the ABS frames works only under conditions of limited contention between nodes. We define the downlink duration for transfer of data traffic from the AP to relays or to their associated nodes (i.e., $AP \rightarrow m_j$ or $AP \rightarrow m_j \rightarrow n_i$) and also corresponding ACKs that traverse the links in the reverse direction. On the other hand, the uplink duration is for data packets originating from the relays or associated nodes, with the AP as the destination. The ACKs in this case also arrive in the opposite direction within the same window of transmission. It is possible that a relay may not have sufficient time to forward data packets that it receives within the same ABS window. In such cases, the relay packet queue grows and transmission resumes the next time the group is assigned the ABS. The contention mechanism within a group is explained in detail later in Section 5.2.

E-Fi defines a load factor for every group j, denoted by η_j, as a weighted expression of $w_{ij}{}^*$ (Eq. (3)) of (i) number of nodes in the group —Ψ_j— and the application load λ_i and μ_i, representing the throughput desired in the downlink (Eq. (6)) and uplink (Eq. (7)), respectively. For Set II, which contains the individual nodes (Ψ_C), we set $w_j = 1$ in the above equations (we assume the AP itself is sufficiently spaced from the LTE BS and not affected by the LTE interference) and $\lambda_{m_j} = 0, \mu_{m_j} = 0$ (no relay is present).

$$\eta_j{}^{DL} = \lambda_{m_j} \cdot w_j + \sum_{\substack{i \ s.t. \\ n_i \in \Psi_j}} \lambda_{n_i} \cdot w_{ij}{}^* \qquad (6)$$

$$\eta_j{}^{UL} = \mu_{m_j} + \sum_{\substack{i \ s.t. \\ n_i \in \Psi_j}} \mu_{n_i} \cdot w_{ji}{}^* \qquad (7)$$

5.1 Inter-ABS Resource Allocation

Each LTE frame has a number of included ABS subframes. Though the Wi-Fi AP cannot influence this number via feedback to the LTE BS, in E-Fi, it can recognize the ABS pattern and knows when such ABS are scheduled. Let the corresponding vector that indicates the presence of the

ABS locations within the LTE frame be given by $\boldsymbol{A}$, with the number of such ABS represented by $|\boldsymbol{A}|$. For instance, $\boldsymbol{A} = [1100001100]$, where 4 subframes are designated ABS in the LTE frame. The AP assigns resources to the groups proportional to the load factor in the Downlink (Eq. (9)) and Uplink (Eq. (8)).

$$|\boldsymbol{A}|_j{}^{UL} = \frac{\eta_j{}^{UL}}{\sum_{j \geq 1} \eta_j{}^{UL} + \eta_C{}^{UL}} \cdot |\boldsymbol{A}|^{UL} \qquad (8)$$

$$|\boldsymbol{A}|_j{}^{DL} = \frac{\eta_j{}^{DL}}{\sum_{j \geq 1} \eta_j{}^{DL} + \eta_C{}^{DL}} \cdot |\boldsymbol{A}|^{DL} \qquad (9)$$

5.2 Intra-ABS Resource Allocation

In this Section, we explain how E-Fi handles collisions and medium contentions within the ABS frame. Such a frame can be allotted for either uplink or downlink, and we separately consider both these situations. The key idea here is that each device uses a slightly shifted carrier sensing start time while accessing the channel depending upon the number of packets in its MAC layer queue and the reliability of the links (PSR). This time shift results in preferential access to the channel for certain stressed nodes who experience growing queues (such as relays) and distant nodes with low PSR (such as non-safe zone nodes without relays).

5.2.1 Downlink

Both the AP and the relay of a group contend for the channel. If the former wins the contention, then the destination is the relay. If the relay wins, then it begins to forward the queued packets to its associated (and downstream) Wi-Fi Direct group members. Through a control parameter α, E-Fi ensures that (i) the AP has enough opportunities to successfully transmit the packets to the relays (link l_1) according to the application load demanded by the Wi-Fi Direct nodes (Eq. (10)), and (ii) relays have priority to forward the packets from the AP to the respective Wi-Fi Direct nodes (link l_2) as soon as they receive them (Eq. (11)). These conditions provide an upper and lower bound for α (Eq. (12)) as follows:

$$\overbrace{\lambda_{m_j} + \sum_{i \in \Psi_j} \lambda_{n_i}}^{\lambda_j} \leq \frac{T_j \cdot \alpha}{T_{tx} \cdot w_j} \qquad (10)$$

$$\frac{T_j \cdot \alpha}{T_{tx} \cdot w_j} \leq \frac{T_j \cdot (1 - \alpha)}{T_{tx} \cdot \overline{w_{ij}{}^*}} \qquad (11)$$

$$\lambda_j \cdot \frac{T_{tx} \cdot w_j}{T_j} \leq \alpha \leq \frac{w_j}{w_j + \overline{w_{ij}{}^*}} \qquad (12)$$

where, $T_j = |\boldsymbol{A}|_j{}^{DL} \cdot 1ms/40ms$, and 40ms is the duration for which a given ABS pattern is active. $\overline{w_{ij}{}^*}$ is the average PSR in a cluster. Moreover, T_{tx} is the expected time for a successful packet transmission with no collisions. This parameter depends on the exponential backoff time, and PKT, which is the time to transmit a packet. The probability that the AP or the relay gets to transmit is given by α and $(1 - \alpha)$, respectively, (Note that $\alpha = 1$ for Set II) and
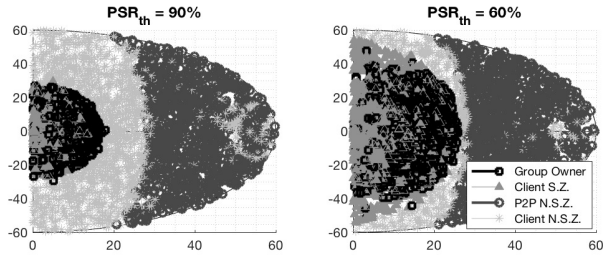
Fig. 9. Node categorization and distribution in the coverage area when different PSR_{th} are selected. As the PSR_{th} decreases, more devices can be elected as relays and hence, serve more devices in the outside the *S.Z.*. The Wi-Fi AP is located at (0,0) and the LTE BS at (60,0).

allows for modifying both the duration of DIFS and the contention window as following Eq. (13). Note that Eq. (12) returns a feasible range if a PSR_{th} is selected following the steps in Sec. 4 and the requirement in Eq. (3) is met.

$$
\begin{aligned}
DIFS_{m_j->n_i} &= (1-\alpha) \cdot DIFS \\
CW_{m_j} &= (1-\alpha) \cdot CW \\
DIFS_{AP->m_j} &= \alpha \cdot DIFS \\
CW_{AP} &= \alpha \cdot CW
\end{aligned}
\tag{13}
$$

5.2.2 Uplink

The uplink consists of two different situations that arise for nodes in Set I and Ψ_C. Consider nodes in Set I, where a relay j and its associated devices $|\Psi_j|$ contend for the channel. E-Fi gives priority to the relay to forward the packets from the Wi-Fi Direct nodes to the AP (Eq. (11)). Thus, the equation 10 is valid with $w_j = 1$ (as the PSR from the relays to the AP is assumed to be 100%) and w_{ji}^* remains the reverse-path PSR in the UL.

For the nodes that belong in Ψ_C and form the Set II, the individual devices outside of the safe zone also contend with others within the safe zone. From Figure 1, we see that the first column of the ABS always carries pilots that may also cause the Wi-Fi clients closer to the LTE BS to persistently backoff, while the ones within the safe zone (and hence farther from the BS) may discover the channel to be free. To address this inequality at both PHY and MAC layers, E-Fi defines a time shifted window for the safe-zone nodes. All nodes that are in the safe zone and member of Set II must wait for 1 resource unit time from the start of the ABS before starting the DIFS. There is no such wait period imposed on the non-safe zone nodes. The intuition here is to give the nodes with low PSR additional opportunities to transmit within the ABS and bring about some measure of fairness in the link throughput for each node. We evaluate this design decision using Jain's fairness index in Sec 6.

6 PERFORMANCE EVALUATION

We evaluate E-Fi using an integrated MATLAB and NS-2 simulation environment. MATLAB is used to model the signal waveforms at the PHY layer that are 100% standards-compliant using WLAN and LTE System toolboxes. This allows studying interference caused by LTE on a per-resource unit basis for various separation distances of Wi-Fi nodes.
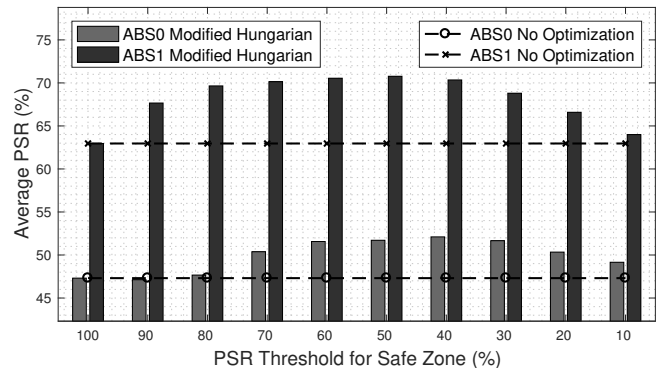

Fig. 10. Average PSR of the Wi-Fi devices when several PSR thresholds are selected defining the Safe Zone. The optimum value lies between 70% and 40%
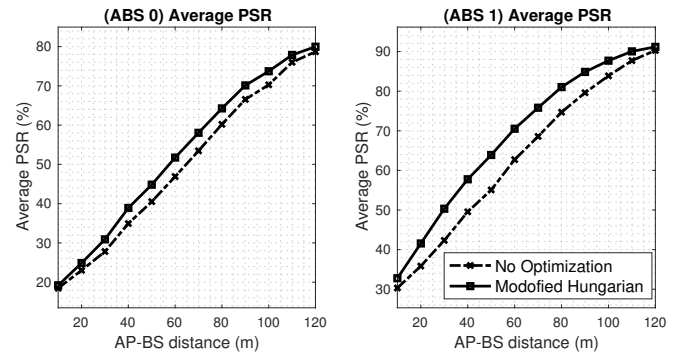

Fig. 11. Average PSR of Wi-Fi devices for different AP-BS distances. The Wi-Fi devices are deployed within the initial Coverage Area, defined to be 90% PSR with no LTE interference. The PSR threshold is chosen to be 70%. E-Fi proves to provide the highest improvement when the BS is located 20-80 meters far from the AP.

The spatiotemporal interference map is then imported into the NS-2 simulator, where we simulate the Wi-Fi Direct group formation and E-Fi's enhanced channel access mechanism.

We first characterize the optimum range of PSR threshold to perceive the maximum improvement from E-Fi for several AP-BS distances. Further, we evaluate the improvement introduced by E-Fi as a function of the distance between the AP-BS aiming to avoid topology restrictions. Knowing that E-Fi performance is tightly related with the number of potential relays, we evaluate E-Fi's performance for several network densities and selected a commercial range. Finally, we perform a broad study on the throughput and Packet Delivery Ratio (PDR) for different network configurations as well as a comprehensive overview of the combined impact of the LTE control signals and channel contention on the Clear Channel Assessments (CCA) embedded in Wi-Fi's DCF.

The simulations performed in this section consider 17dBm to be the transmit power for both Wi-Fi-AP and BS-LTE, which is the maximum transmit power output per antenna in the 802.11n standards for indoor communications in this band. Furthermore, the initial coverage area is selected as for to provide 90% PSR when no LTE interference is present. Commercial deployments require PER levels within
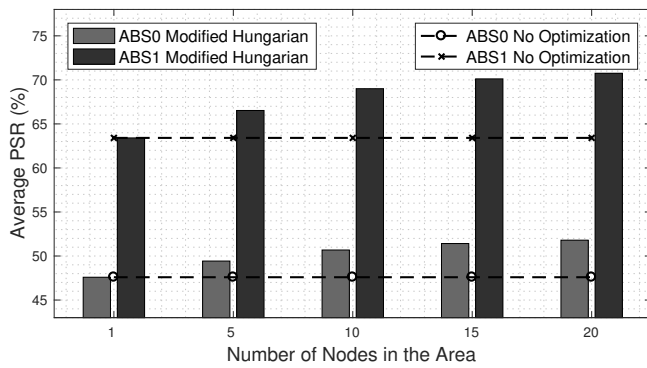
Fig. 12. Average PSR of Wi-Fi devices when different number of Wi-Fi devices are deployed in the network. The PSR threshold is chosen to be 70%. E-Fi always improves the PSR and achieves a maximum of 10% improvement.

the range of 10-30% to provide reliable and uninterrupted communication without affecting the user experience. The initial Wi-Fi transmit rate was configured to be MCS-3 (16-QAM with coding rate 1/2) with enabled automatic rate fallback (ARF).

For space reasons, we report only the results referred to as downlink traffic scenario, i.e. the AP generates equal Constant Bit Rate (CBR) traffic for all Wi-Fi nodes given by λ pkts/s. Let T_{share} be the temporal share of the channel usage between the LTE and the Wi-Fi network, depending on how many ABS frames are included (it is impossible for Wi-Fi to operate in LTE data frames). Since E-Fi works in uncooperative LTE deployments, the value of T_{share} is tunable.

6.1 PSR threshold selection in E-Fi

The Safe Zone, directly defined by the PSR threshold, determines the number of nodes that could become Group Owners. As the PSR threshold decreases, more devices could meet the criteria and be elected as a Group Owner by the AP. Figure 9 shows how the PSR threshold determines the relay roles, and defines the regions outside the Safe Zone where nodes are most likely to be assigned a relay to increase their PSR. As the PSR threshold decreases, the Safe Zone area widens, more devices are categorized as Group Owners and, in turn, more nodes outside the Safe Zone can relayed. Also, Figure 9 shows that the devices elected as W-Fi direct clients are the ones closest to the LTE-BS, and thus suffering from severe interference. However, there is a small set of nodes, the closest one to the BS, for which E-Fi cant find an improvement given the high levels of interference.

Figure 10 shows the optimum value for the PSR threshold so that E-Fi provides the maximum PSR. The optimum range is defined as the one that provides the highest average PSR for the considered AP-BS distance. The modified Hungarian Algorithm finds the maximum average PSR when the threshold is selected within the range 40-70%, where the AP has enough Group Owners, and nodes with low PSR that lie outside the Safe Zone become Wi-Fi Direct Clients. The node distribution is shown in Figure 16.
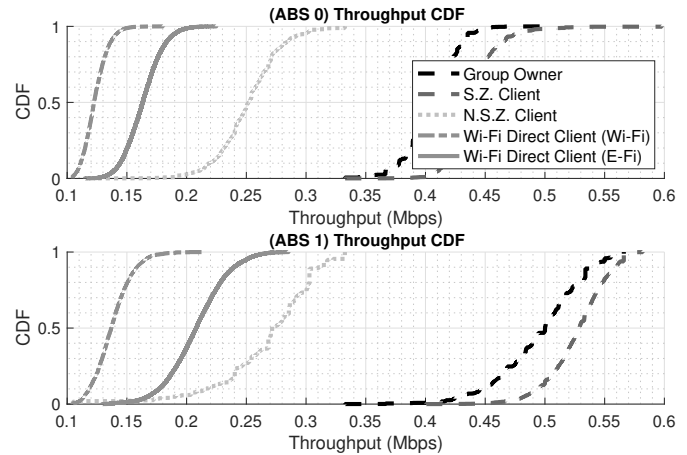

Fig. 13. CDF of the Throughput of the Wi-Fi devices when 20 devices are operating in the network, the PSR threshold is chosen to be 70% and the BS is located 60m far from the AP. E-Fi improves the PHY throughput of the Wi-Fi Direct Clients 50-70%. Sec. 6 describes the communication set-up, i.e. deployment scenario, transmit power and PSR_{th}.

6.2 Impact of the distance between the AP and BS

Since we consider the transmit power to be fixed to the maximum, we evaluate E-Fis performance for different AP-BS distances. Figure 11 depicts the range where the maximum improvement is reached. The node distribution is shown in Figure 16. As expected, when no LTE interference is present, the average PSR converges to the initial PSR threshold defining the coverage area.

6.3 Impact of the number of Wi-Fi devices

E-Fi relies on a certain number of nodes perceiving high PSR so that by enabling relaying capabilities, the PSR of other nodes can be increased. Figure 12 shows the PSR change as the number of nodes increases. The node distribution is shown in Figure 16. Note that the increasing trend is because the PSR metric does not consider the impact of the channel availability or collisions, but it just accounts for the reliability of the link against LTE interference.

6.4 PHY throughput improvement introduced by E-Fi

Next, we evaluate the improvement on the average PHY throughput that Wi-Fi Direct clients perceive by employing relaying capabilities. Figure 13 shows the throughput distribution for a network where 20 Wi-Fi devices operating within the coverage area being interfered by an LTE-BS located 60m far from the AP. The PSR threshold is chosen to be 70%.We note few key findings: First, E-Fi introduces 50-70% improvement on the throughput of the nodes affected by the LTE interference. Second, the Group Owners tend to have lesser PSR than the Safe Zone Clients, meaning they are located closer to the Safe Zone boundary. Third, E-Fi helps the devices that are most affected by the LTE interference.

6.5 MAC-based analysis of E-Fi - impact on the CCA

While other proposals that use duty cycling, such as LTE-U, require a wider time window for the Wi-Fi devices to
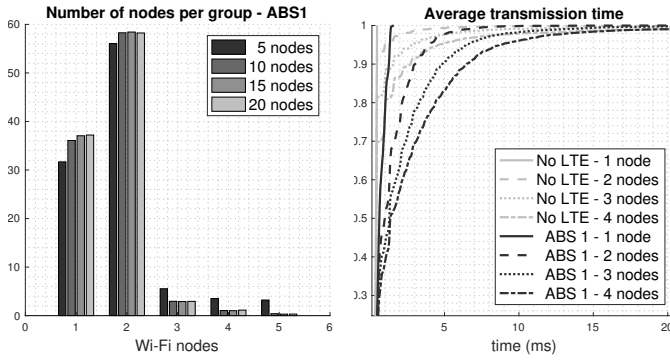
Fig. 14. Dimensionality of the E-Fi groups for ABS 1. Roughly 95% of the groups end up having between 1 and 3 devices.

Fig. 15. Transmission time accounting for the LTE control signals and the contention between the Wi-Fi nodes.
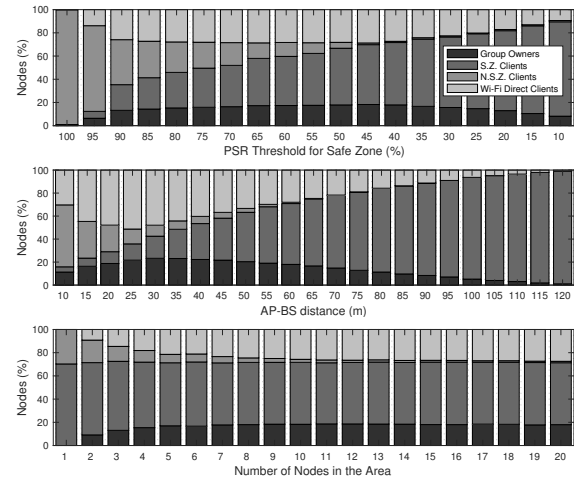

Fig. 16. Analysis of the Statistical Role distribution of Wi-Fi nodes when subframe 1 is designated ABS when we vary the PSR threshold defining the Safe Zone, the distance between the AP and the BS in meters, and the number of Wi-Fi nodes operating in the network. Default values are $PSR_{th} = 0.6$, AP-BS distance $= 50$ (m) and 20 Wi-Fi nodes

transmit, E-Fi shortens the available transmission time by clustering the devices into groups and allocating few ABS to each of them. Figure 14 shows a statistical distribution of nodes per E-Fi group, proving that groups contain between one and three nodes roughly 95% of the times. Figure 15 shows the average time to successfully transmit a packet for different group sizes, accounting for the impact of the LTE control signals on the CCA carried out in the DCF. In short, the grouping mechanism allows for the reduction of the time given to Wi-Fi to transmit down to a few milliseconds (ABS subframes).

6.6 Benefits of Traffic Forwarding via Relays

We next evaluate how relays improve the application layer Packet Delivery Ratio (PDR) by comparing five different schemes with modular enhancements:

- *LTE OFF, Legacy Wi-Fi.* No interference is present in this configuration (Blank Subframes). Used as a baseline comparison.
- *LTE ON, Legacy Wi-Fi.* LTE interference is characterized by the Matlab results in section 3.1. Realistic and current scenario.
- *LTE ON, Random WiFi relay selection.* The system groups the nodes based on a random pattern.
- *LTE ON, Random WiFi relay selection over the Relay Candidate (RC) set.* The pairing follows the Eq. (3), where the candidates must lay within the Safe Zone.
- *LTE ON, Hungarian-based WiFi relay selection.* The system groups the nodes according to the modified Hungarian algorithm (section 4.4).

The parameters under study for this section are: $Nnodes$, representing the number of Wi-Fi nodes; T_{share}, denoting the time ratio assigned to Wi-Fi (i.e. the LTE and WI-FI networks have equal share when $T_{share} = 50\%$); and λ, representing the Wi-Fi traffic rate in packets per second. Figure 17(a) shows the impact of the $Nnodes$, from which we can draw some conclusions. First, the LTE OFF case overestimates data delivery without capturing packet losses. Second, the legacy Wi-Fi incurs up to 60% of packet losses for $Nnodes$=20, primarily due to: (*i*) channel errors caused by the BS interference or (*ii*) buffer overflow at the AP. Third, The pure random selection scheme worsens the

situation due to the inefficient relay selection and may end up lowering the quality of the link. Finally and despite of the fact that the random grouping over the RC scheme equally distributes the nodes amongst Wi-Fi Direct groups, the Hungarian-based algorithm maximizes the probability of successful data delivery (20% or more compared to the legacy Wi-Fi) by also taking into account the quality of each wireless link. The same improvement was observed for the network throughput, which was not included due the shortage of space.

Figure 17(b) shows the impact of the T_{share} on the average PDR. Regardless of the configuration, the performance increases as T_{share} increases due the higher chances to access the channel. For the case LTE OFF, the system experience some packet dropping at $T_{share} \leq 33\%$ due to buffer overflow at the AP. These results confirm that the Hungarian Algorithm approach maximizes the performance, with an improvement of 31% PDR compared to the legacy Wi-Fi for T_{share}=75%. The same conclusions can be derived from Figure 17(c), where we show the average PDR as a function of λ.

6.7 ABS Resource Allocation Network Analysis

A comprehensive analysis of the resource allocation mechanism introduced in E-Fi is presented in this section. The schemes being compared are:

- *Legacy Wi-Fi*, i.e. the current practical systems deployed today.
- *The Hungarian-based relay selection*, using the legacy 802.11-DCF at the MAC layer.
- *E-Fi framework*, where both the Hungarian-relay selection (section 4.3 and 4.4) and the ABS allocation algorithm (section 5) are employed with differentiated contention access.

Figure 18(a) shows the average PDR for the three schemes. We see that (*i*) the ABS allocation algorithm provides a significant improvement to the performance of E-Fi, which
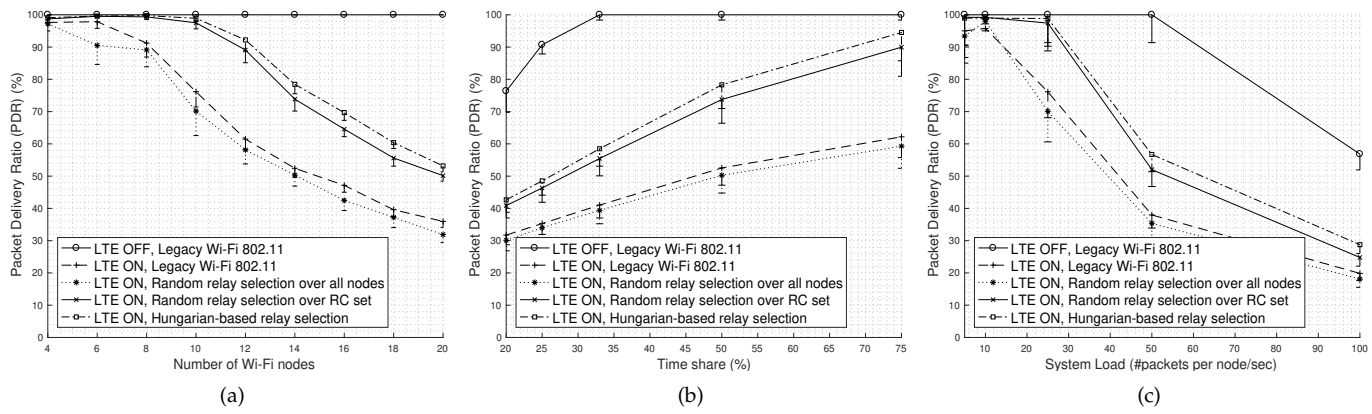
Fig. 17. Impact of $Nnodes$ (a), T_{share} (b), and λ (c) on the PDR . The default values are $Nnodes = 10$, $T_{share} = 50\%$ and $\lambda = 25$)
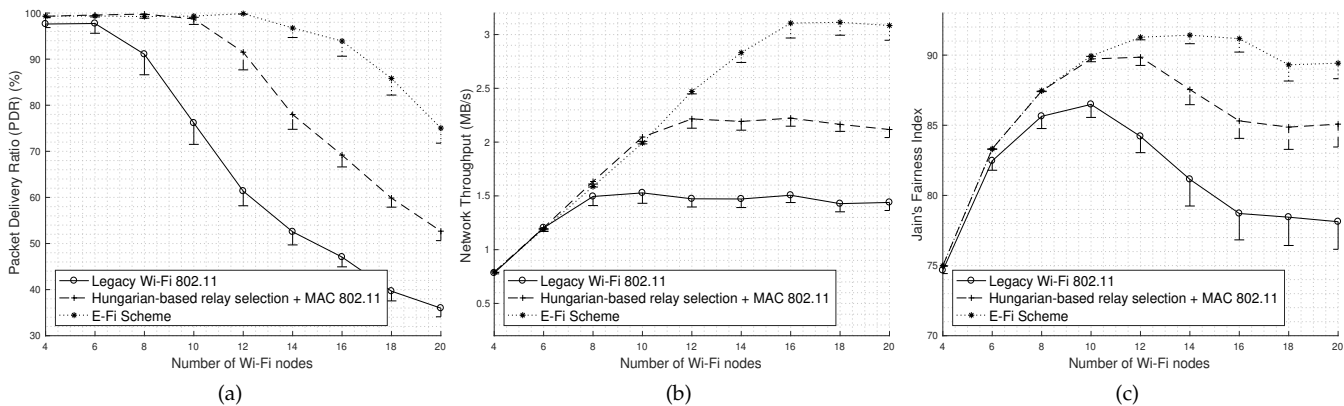

Fig. 18. Impact of the configuration schemes (section 6.7) on the PDR (a), throughput (b) and Jain's fairness index (c). The default values are $T_{share} = 50\%$ and $\lambda = 25$)

now outperforms the legacy Wi-Fi standard by almost 100% percent in highly dense scenarios (i.e. N=20); (*ii*) even in these extreme situations, the PDR of E-Fi gets considerably close to the baseline reference (LTE OFF in Figure 18(a)), with only 20% difference in terms of PDR. Hence we argue that the Wi-Fi network can really survive LTE-U using E-Fi, mitigating most of the interference coming from the BS. The same inference can be derived in terms of throughput shown in Figure 18(b).

Finally, Figure 18(c) shows the throughput fairness among the N data flows, computed using the well-known Jain's Fairness index. Also in this case, E-Fi provides the best performance because: (*i*) the Hungarian-relay selection mechanism guarantees average higher link quality for vulnerable clients; (*ii*) the inter-ABS scheduler allocates channel opportunities in a fair way based on the load factor of each Wi-Fi Direct group (Eq. (6)); (*iii*) the intra-ABS scheduler adjusts the MAC back-off parameters so that the AP and the relay will have proportional channel access during each ABS.

6.8 Case in point: E-Fi vs LTE-U

Efforts to standardize LTE in the unlicensed spectrum have resulted in two main implementation proposals, Licensed-Assisted Access (LAA) that is supported by 3GPP and defined in Release 13 as part of its work plan for 5G

[41], and LTE-U from LTE-U Forum that is based on 3GPP Releases 10/11/12 [42]. Both proposals envision considerable changes to currently deployed LTE specifications. LAA manages access to the unlicensed spectrum using a Listen-Before-Talk (LBT) scheme that resembles CSMA/CA and exploits carrier-aggregation to anchor unlicensed band access to it to a licensed band, while LTE-U adopts a Carrier Sense Adaptive Transmission (CSAT) as mechanism deployed on Secondary Cell (SCell) in the downlink, and employs an on/off duty cycle as a mechanism to share the medium with existing Wi-Fi networks.

As opposed to LTE-U and LAA, E-Fi groups WiFi devices as to minimize the expected number of transmissions $(1/PSR)$ and further allocates transmission time to them based on the result and their application load (pkts/s). E-Fi inherently relies on the ABS distribution that LTE previously configured to fulfill its own interference requirements, binding its performance to the available number of ABS.

Comparison has been made also against LTE-U with duty cycling considering the default 80ms value[43]. It has been shown in [44] that LBT(LAA) and CSAT(LTE-U) converge for sufficiently long LTE transmissions, and a choice of either is mainly driven by LTE operators interests. Therefore, we analyzed the average required time (in ms) for a determined number of Wi-Fi nodes to access the channel and successfully complete a transmission. Results are shown
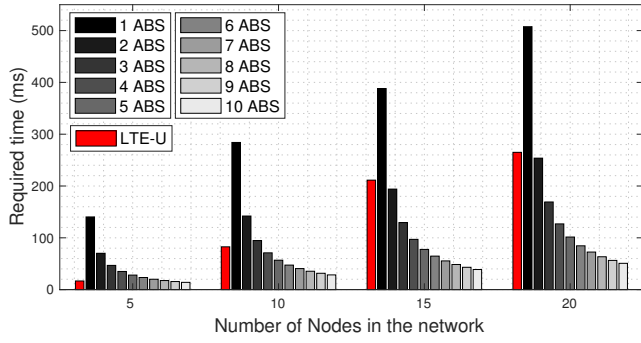
Fig. 19. Latency comparison between LTE-U, with Ton/off equal to 80ms, and E-Fi with equal load factor across the nodes. E-Fi performance depends on the number of available ABS to schedule its transmissions. E-Fi outperforms LTE-U when the number of Wi-Fi nodes is greater or equal than 10. As the number of nodes increases, E-Fi requires less ABS to outperform LTE-U. Thus, proving the effectivity of the grouping and resource allocation mechanisms proposed in E-Fi.
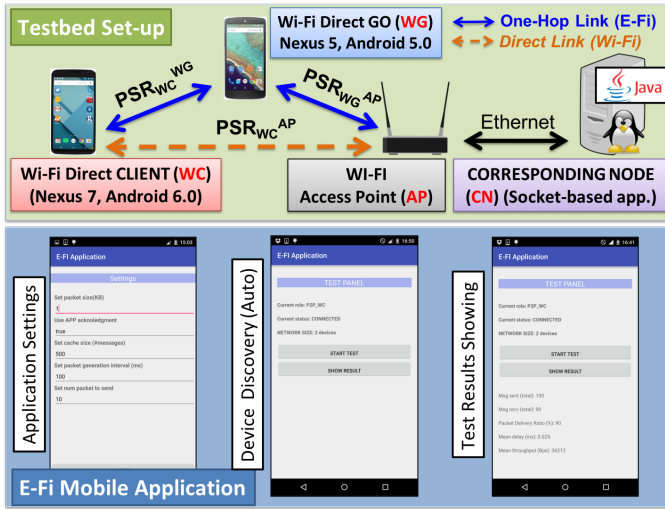

Fig. 20. Experimental set-up in Section 7. The WC is constituted by a Nexus 6 smartphone running Android 6.0 Operating System (OS), and the GO is a Nexus 5 smartphone running Android 5.0 OS (above). An Android application is installed on the WC and GO and implements the procedures described in Sections 4 and 5.

in Figure 19 for different network sizes and all the possible ABS configurations (1 to 10 ABS available). Load is evenly distributed among all the Wi-Fi devices.

7 TESTBED AND EXPERIMENTAL RESULTS

In this Section, we evaluate the performance of E-Fi on a small-case testbed. More specifically, our goal is to demonstrate that E-Fi is able to improve the performance of Wi-Fi nodes under several different network topologies and LTE interference levels in spite the overhead introduced by Wi-Fi Direct and the one-hop communication. To this aim, we built the testbed composed of four nodes: one Wi-Fi Direct Client (WC); one legacy IEEE 802.11 AP; one Corresponding node (CN) connected to the AP via Ethernet; and a Wi-Fi Direct GO (GO), which forwards the traffic from the WC to the CN via AP (Figure 20). The WC node generates a constant number of UDP packets per second (κ); the packet size
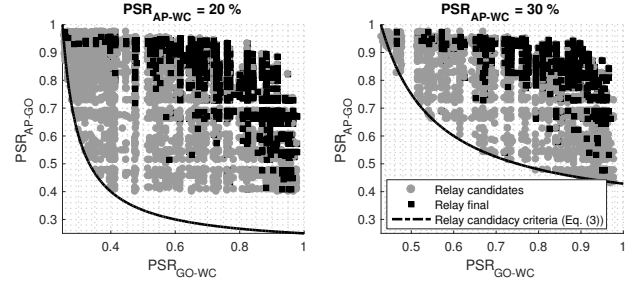

Fig. 21. Relay candidacy and final relay selection in a deployment with 20 devices, BS-AP distance of 50m and PSR_{th} equal to 0.4. The PSR_{AP-WC} represents the link quality of the regular Wi-Fi communication whereas PSR_{AP-GO} and PSR_{GO-WC} represent the link quality in E-Fi. The inner area delimited by the line represents the feasible set, meeting the criteria in Eq. (3). The Hungarian always selects the combination with highest PSR.

is equal to 1000 bytes. The LTE interference was modeled with the PSR and is denoted as PSR_{WC}^{AP}, on the WC-AP link; PSR_{WC}^{GO} on the WC-GO link; and PSR_{GO}^{AP} on the GO-AP link. The PSR values were extracted from a feasible set of combinations (i.e. Figure 21 shows the feasible set when PSR_{WC}^{AP} is 20% and 30%) Therefore, we devised two communication scenarios:

- *C1 - No-Relay*: The WC sends the packets directly to the CN (state-of-the-art Wi-Fi).
- *C2 - Relay*: The WC first transmits to the GO, which forwards it to the CN afterwards.

Performance metrics, such as the network throughput, the PDR and the delay were extracted upon completion and displayed on the Application GUI. Notice that processes such as network set-up, i.e. the PSR exchange, device discovery and role selection are handled by the E-FI mobile application (Figure 20). Figure 22(a) shows the achievable throughput accounting for the overhead incurred in *C2* by the GO node for 3 baseline scenarios ($PSR_{WC}^{AP} = 60\%, 40\%, 20\%$). Since *C1* is independent from the relay, the results are constant across the x plane. We selected reasonable set of values for PSR_{WC}^{GO} (Figure 21) while keeping κ constant at 300. The regions when configuration *C2* outperforms *C1* correspond to those in the graph where the curves lay above the baseline.

The PDR (Figure 22(b)) gives us a direct metric of the performance accounting for retransmissions. Similar to the throughput analysis, E-Fi perceives a better PDR than Wi-Fi in certain cases. For instance, given the combination PSR_{WC}^{AP}=20%, PSR_{WC}^{GO}=80%, PSR_{GO}^{AP}=80% (feasibility shown in Figure 21), E-Fi raises the PDR from 20% to almost 60%. As a conclusion, we notice that the one-hop communication is suitable for moderate or severe interference conditions (i.e. PSR_{WC}^{AP}=20% and PSR_{WC}^{AP}=40%), verifying the simulation analysis in Section 6.1.

In Figure 22(c), we show the throughput gain of the E-Fi scheme, considering κ=300 and severe LTE interference conditions (PSR_{WC}^{AP}=20%), and by varying the PSR_{WC}^{GO} parameter (on the x-axis), and the PSR_{GO}^{AP} parameter (on the y-axis). The gain is computed as the throughput increase (in percentage) compared to the no-relay scheme. In our implementation, E-Fi employs the utilization of the GO relay
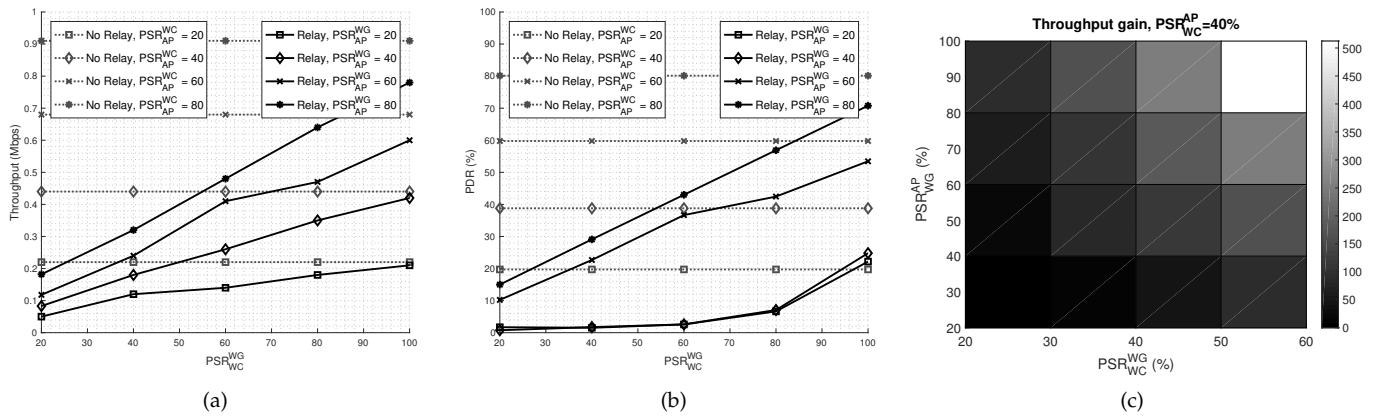
(a) (b) (c)

Fig. 22. Testbed results. The network throughput and PDR for different configurations of PSR_{WC}^{AP} and PSR_{WC}^{GO} are depicted in (a) and (b), respectively. The E-Fi throughput gain is depicted in (c)

only when the PSR condition in Eq. (3) is met; otherwise, the WC will transmit data directly to the CN as in the no-relay scheme (hence achieving a zero gain in these cases). From Figure 22(c), we notice that the throughput gain can exceed the +500% under some configurations, with a mean value of +85%.

Aiming to provide some metrics on the incurred delay by the multi-hop communication, we configure *C1* and *C2* with different system loads and evaluate the PDR and delay jointly (Figure 23). We consider a configuration with PSR_{WC}^{GO}=80%, PSR_{GO}^{AP}=80% and PSR_{GO}^{WC}=20%. The PDR results reveal that E-Fi always outperforms Wi-Fi for any system load. Vice versa, E-Fi introduces a higher delay than Wi-Fi, although the values are quite close for any system load. Several factors need to be considered when interpreting this result. Fist, delay measurements only consider packets that were received successfully, and hence are clearly affected by the congestion issues which might originate at the GO device. E-Fi is able to successfully deliver a considerably higher ratio of packets, and this also implies that each packet experience -on average- a longer buffer delay at the queue of the intermediate GO relay. Second, the experiment set-up serves for an understanding of the delayed incurred by the LTE control signals and in the relay node. However, it does not consider the delay incurred due to the contention amongst Wi-Fi devices (actually only one WC device is considered).

In accordance with the analysis covered in Section 6.8, the E-Fi produces an effective performance gain in terms of delay when the number of WC is higher than a threshold which depends on the number of ABS (see Figure 19). Finally, it is worth remarking that the current testbed implements the E-Fi functionalities at the application layer; hence, each message forwarding operation incurs in an additional processing delay, which might be nullified when deploying the E-Fi scheme at the MAC layer.

8 CONCLUSION

We proposed E-Fi, which allows Wi-Fi devices to survive uncoordinated LTE transmissions through grouping of nodes into relays, separating Uplink/Downlink traffic durations and modifications to the backoff based on PSR.
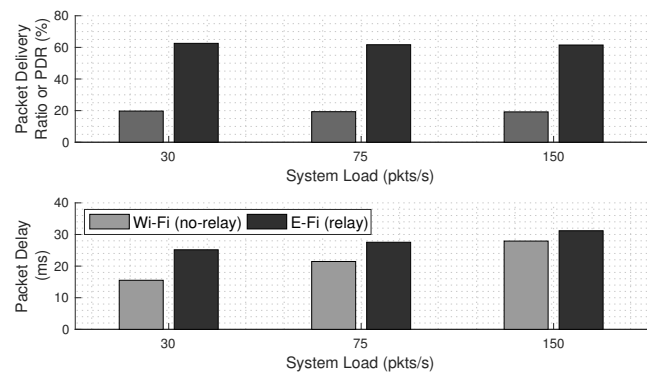

Fig. 23. Delay incurred by the direct and one-hop communication for different system loads. Although E-Fi may incur in a higher communication delay, it lowers the probability of dropping and, in turn, increases the PDR.

Our design is motivated through studies conducted with real devices, network simulators and standards-compliant LTE and WLAN physical layer waveforms. We show for the first time that Wi-Fi can intelligently adapt its operation to handle high PER and lack of channel access opportunities through the use of ABS frames. Through a mix of packet-level simulation using a standards-compliant physical layer, as well as testbed experiments, we show that E-Fi's improvements over classical Wi-Fi range from 25-50% for throughput and 15% for PER under severe interference from LTE. We also provide a comprehensive comparison between E-Fi and LTE-U, the strongest proposal to be included in the next release, as well as conditions under which E-Fi outperforms LTE-U. Given the involvement of P2P device querying and the required measurement exchange with the AP, E-Fi is more applicable in low-mobility scenarios. Our work demonstrates that it is indeed possible to coexist without assumptions of direct feedback between these two very different access technologies in the ISM band. The multiple AP scenario where the APs operate in the same channel is being investigated and will be incorporated in future work. We are evaluating a game theory-based approach that will allow E-Fi APs to select the channel in multi-AP scenario. We are also considering cases where more than one LTE station shares the spectrum.
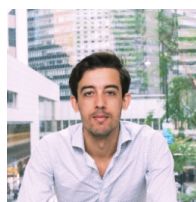
ACKNOWLEDGMENTS

REFERENCES

[1] Cisco, "Global Mobile Data Traffic Forecast Update, 2015-2020 White Paper. Accessed on 18 April 2016."

[2] A. M. Cavalcante, E. Almeida, R. D. Vieira, S. Choudhury, E. Tuomaala, K. Doppler, F. Chaves, R. C. Paiva, and F. Abinader, "Performance evaluation of LTE and Wi-Fi coexistence in unlicensed bands," in *IEEE VTC, 2013*, pp. 1–6.

[3] E. Almeida, A. M. Cavalcante, R. C. Paiva, F. S. Chaves, F. M. Abinader, R. D. Vieira, S. Choudhury, E. Tuomaala, and K. Doppler, "Enabling LTE/WiFi coexistence by LTE blank subframe allocation," in *IEEE ICC, 2013*, pp. 5083–5088.

[4] S. Sesia, I. Toufik, and M. Baker, *LTE, The UMTS Long Term Evolution: From Theory to Practice*. Wiley Publishing, 2009.

[5] Wi-Fi Alliance, "Wi-Fi peer-to-peer (P2P) technical specification," *www. wi-fi. org/Wi_Fi_Direct. php*, 2010.

[6] A. Babaei, J. Andreoli-Fang, Y. Pang, and B. Hamzeh, "On the impact of LTE-U on Wi-Fi performance," *International Journal of Wireless Information Networks*, vol. 22, no. 4, pp. 336–344, 2015.

[7] H. Zhang, X. Chu, W. Guo, and S. Wang, "Coexistence of Wi-Fi and heterogeneous small cell networks sharing unlicensed spectrum," *IEEE Communications Magazine*, vol. 53, no. 3, pp. 158–164, 2015.

[8] C. Cano and D. J. Leith, "Coexistence of WiFi and LTE in unlicensed bands: A proportional fair allocation scheme," in *IEEE ICCW*, 2015, pp. 2288–2293.

[9] A. K. Sadek, "Carrier sense adaptive transmission (csat) in unlicensed spectrum," Nov. 8 2016, uS Patent 9,491,632.

[10] N. Rupasinghe and İ. Güvenç, "Reinforcement learning for licensed-assisted access of lte in the unlicensed spectrum," in *Wireless Communications and Networking Conference (WCNC), 2015 IEEE*. IEEE, 2015, pp. 1279–1284.

[11] Z. Guan and T. Melodia, "CU-LTE: Spectrally-efficient and fair coexistence between LTE and Wi-Fi in unlicensed bands," in *IEEE INFOCOM, 2016*.

[12] T. Tao, F. Han, and Y. Liu, "Enhanced lbt algorithm for lte-laa in unlicensed band," in *Personal, Indoor, and Mobile Radio Communications (PIMRC), 2015 IEEE 26th Annual International Symposium on*. IEEE, 2015, pp. 1907–1911.

[13] S. Hajmohammad, H. Elbiaze, and W. Ajib, "Fine-tuning the Femtocell performance in unlicensed bands: Case of WiFi Coexistence," in *IEEE IWCMC, 2014*, pp. 250–255.

[14] F. Liu, E. Bala, E. Erkip, and R. Yang, "A framework for femtocells to access both licensed and unlicensed bands," in *IEEE WiOpt, 2011*, pp. 407–411.

[15] Y. Li, J. Zheng, and Q. Li, "Enhanced listen-before-talk scheme for frequency reuse of licensed-assisted access using lte," in *Personal, Indoor, and Mobile Radio Communications (PIMRC), 2015 IEEE 26th Annual International Symposium on*. IEEE, 2015, pp. 1918–1923.

[16] S. Nielsen and A. Toskala, "LTE in unlicensed spectrum: European regulation and co-existence considerations," in *3GPP workshop on LTE in unlicensed spectrum, Sophia Antipolis, France*, 2014.

[17] S. Deb, P. Monogioudis, J. Miernik, and J. P. Seymour, "Algorithms for enhanced inter-cell interference coordination (eICIC) in LTE HetNets," *IEEE/ACM Transactions on Networking (TON)*, vol. 22, no. 1, pp. 137–150, 2014.

[18] J. Jeon, Q. C. Li, H. Niu, A. Papathanassiou, and G. Wu, "LTE in the unlicensed spectrum: A novel coexistence analysis with WLAN systems," in *IEEE GLOBECOM, 2014*, pp. 3459–3464.

[19] S. Sagari, S. Baysting, D. Saha, I. Seskar, W. Trappe, and D. Raychaudhuri, "Coordinated dynamic spectrum management of LTE-U and Wi-Fi networks," in *IEEE DySPAN, 2015*, pp. 209–220.

[20] A. Bhorkar, C. Ibars, and P. Zong, "On the throughput analysis of LTE and WiFi in unlicensed band," in *IEEE 48th Asilomar Conference on Signals, Systems and Computers, 2014*, pp. 1309–1313.

[21] A. M. Voicu, L. Simić, and M. Petrova, "Inter-technology coexistence in a spectrum commons: A case study of wi-fi and lte in the 5-ghz unlicensed band," *IEEE Journal on Selected Areas in Communications*, vol. 34, no. 11, pp. 3062–3077, 2016.

[22] A. Pyattaev, K. Johnsson, S. Andreev, and Y. Koucheryavy, "3GPP LTE traffic offloading onto WiFi Direct," in *IEEE WCNCW, 2014*, pp. 135–140.

[23] A. Asadi, P. Jacko, and V. Mancuso, "Modeling D2D communications with LTE and WiFi," *ACM SIGMETRICS Performance Evaluation Review*, vol. 42, no. 2, pp. 55–57, 2014.

[24] D. M. Gutierrez-Estevez, B. Canberk, and I. F. Akyildiz, "Spatiotemporal estimation for interference management in femtocell networks," in *2012 IEEE 23rd International Symposium on Personal, Indoor and Mobile Radio Communications - (PIMRC)*. IEEE, 2012, pp. 1137–1142.

[25] J. Xie and I. Howitt, "Multi-domain wlan load balancing in wlan/wpan interference environments," *IEEE Transactions on Wireless Communications*, vol. 8, no. 9, pp. 4884–4894, 2009.

[26] A. Asadi and V. Mancuso, "WiFi Direct and LTE D2D in action," in *Wireless Days (WD), 2013 IFIP*. IEEE, 2013, pp. 1–8.

[27] G. A. Shah, F. Alagoz, E. A. Fadel, and O. B. Akan, "A Spectrum-aware Clustering for Efficient Multimedia Routing in Cognitive Radio Sensor Networks," *IEEE Transactions on Vehicular Technology*, vol. 63, no. 7, pp. 3369–3380, 2014.

[28] B. Gulbahar and O. B. Akan, "Information Theoretical Optimization Gains in Energy Adaptive Data Gathering and Relaying in Cognitive Radio Sensor Networks," *IEEE Transactions on Wireless Communications*, vol. 11, no. 5, pp. 1788–1796, 2012.

[29] P. Series, "Propagation data and prediction methods for the planning of indoor radiocommunication systems and radio local area networks in the frequency range 900 MHz to 100 GHz," *Recommendation ITU-R*, pp. 1238–7, 2012.

[30] I. Gomez-Miguelez, A. Garcia-Saavedra, P. D. Sutton, P. Serrano, C. Cano, and D. J. Leith, "srslte: an open-source platform for lte evolution and experimentation," pp. 25–32, 2016.

[31] A. Tirumala, F. Qin, J. Dugan, J. Ferguson, and K. Gibbs, "Iperf: The TCP/UDP bandwidth measurement tool," *http://dast.nlanr.net/Projects*, 2005.

[32] Atheros Communications Inc., "Drivers for Atheros IEEE 802.11n PCI/PCI-Express and AHB WLAN based chipsets," https://wireless.wiki.kernel.org/en/users/drivers/ath9k, 2016.

[33] R. Krishnakumar, "Kernel korner: kprobes-a kernel debugger," *Linux Journal*, vol. 2005, no. 133, p. 11, 2005.

[34] C. Chekuri and S. Khanna, "A polynomial time approximation scheme for the multiple knapsack problem," *SIAM Journal on Computing*, vol. 35, no. 3, pp. 713–728, 2005.

[35] H. W. Kuhn, "The Hungarian method for the assignment problem," *Naval research logistics quarterly*, vol. 2, no. 1-2, pp. 83–97, 1955.

[36] V. Liu, A. Parks, V. Talla, S. Gollakota, D. Wetherall, and J. R. Smith, "Ambient backscatter: Wireless communication out of thin air," in *Proceedings of the ACM SIGCOMM 2013 Conference on SIGCOMM*, ser. SIGCOMM '13. New York, NY, USA: ACM, 2013, pp. 39–50.

[37] S. M. Kim and T. He, "Freebee: Cross-technology communication via free side-channel," in *Proceedings of the 21st Annual International Conference on Mobile Computing and Networking*, ser. MobiCom '15. New York, NY, USA: ACM, 2015, pp. 317–330.

[38] Z. Chi, Z. Huang, Y. Yao, T. Xie, H. Sun, and T. Zhu, "Emf: Embedding multiple flows of information in existing traffic for concurrent communication among heterogeneous iot devices," in *IEEE INFOCOM, 2017*, New York, NY, USA, 2017, pp. 1494–1502.

[39] X. Guo, X. Zheng, and Y. He, "Wizig: Cross-technology energy communication over a noisy channel," in *IEEE INFOCOM, 2017*, New York, NY, USA, 2017, pp. 1485–1493.

[40] D. H. Staelin, "Fast folding algorithm for detection of periodic pulse trains," *Proceedings of the IEEE*, vol. 57, no. 4, pp. 724–725, 1969.

[41] 3GPP, "3GPP 36.889," http://www.3gpp.org/ftp/specs/archive/36_series/36.889/36889-d00.zip.

[42] LTE-U Forum, "LTE-U SDL Coexistence Specifications v1.3," http://www.lteuforum.org/uploads/3/5/6/8/3568127/lte-u_forum_lte-u_sdl_coexistence_specifications_v1.3.pdf.

[43] W.-F. Alliance, "Coexistence guidelines for lte in unlicensed spectrum studies," *V1. 0, Nov*, 2015.

[44] C. Cano and D. J. Leith, "Unlicensed lte/wifi coexistence: Is lbt inherently fairer than csat?" in *Communications (ICC), 2016 IEEE International Conference on*. IEEE, 2016, pp. 1–6.

Carlos Bocanegra received his Bachelor's degree from Polytechnic University of Catalonia (UPC), Barcelona, Spain, in 2015. He is a PhD Candidate in the Electrical and Computer Engineering department at Northeastern University. He was a visiting scholar at Northeastern University from October 2014 to July 2015. His research interests include mobile communications, millimeter waves communications, software-defined radios (SDR), optimum scheduling mechanisms and network slicing.
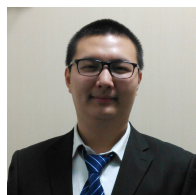
Takai Eddine Kennouche graduated from The National Preparatory School for Engineering Studies of Algiers, Algeria, in 2010 and obtained his Master's degree in Telecommunications Engineering in 2013 from the National Institute of Telecommunications and ICT of Oran, Algeria. He is currently a PhD candidate in the department of Industrial and Information Engineering at the University of Pavia, Italy. His research interests include coexistence of heterogeneous wireless networks, cross layer optimizations, cognitive radio and SDR.

Zhengnan Li received his Bachelor's degree in Communication Engineering from Shandong University of Technology, Zibo, China. He is currently working toward his MS degree in Electrical and Computer Engineering at Northeastern University, Boston, MA. His research interests include wireless communications, 5G and SDR.

Lorenzo Favalli graduated in Electronic Engineering form Polytechnic University of Milan in March 1987 and obtained the PhD from the same university in 1991. He joined the University of Pavia in 1991 as Assistant Professor and became Associate Professor in 2000. His teaching duties include courses of Digital Communications, Wireless Communications Systems and Multimedia Communications. The research activity of Prof. Favalli covers various aspects of signal and video analysis and transmission in both wireless and wired networks. His work also encompasses the exploitation of adaptive techniques to improve flexibility and reliability of the communications chain, source and network modeling and improvements in signal detection techniques in heterogeneous wireless environments.

Marco Di Felice received the Laurea (summa cum laude) and Ph.D. degrees in Computer Science from the University of Bologna, Italy, in 2004 and 2008, respectively. In 2007, he was a visiting researcher with the Broadband Wireless Networking Laboratory, Georgia Institute of Technology, Atlanta, GA, USA. In 2009, he was a visiting researcher with Northeastern University, Boston, MA, USA. Currently, he is an Associate Professor in Computer Science with the University of Bologna. His research interests include self-organizing wireless networks, cognitive radio and vehicular systems, mobile applications and services. Prof. Di Felice currently serves on the editorial board of Elseviers Ad Hoc Networks journal. He authored more than 80 papers on wireless and mobile systems. He joint several national and international research projects. He received the Best Paper Award at the Association for Computing Machinery International Symposium on Mobility Management and Wireless Access (MOBIWAC) in 2012 and at the IEEE Annual Mediterranean Ad Hoc Networking Workshop (MED-HOC- NET) in 2013.

Kaushik Chowdhury (M09SM15) received the PhD degree from the Georgia Institute of Technology, Atlanta, in 2009. He is currently Associate Professor and Faculty Fellow in the Electrical and Computer Engineering Department at Northeastern University, Boston, MA. He was awarded the Presidential Early Career Award for Scientists and Engineers (PECASE) in Jan. 2017, the DARPA Young Faculty Award in 2017, the Office of Naval Research Director of Research Early Career Award in 2016, and the National Science Foundation (NSF) CAREER award in 2015. He received multiple best paper awards, including three in the IEEE ICC conference, in 2009, 12 and 13, and ICNC conference in 2013. He serves on the editorial board of the IEEE Transactions on Wireless Communications, His research has been supported by the NSF, Office of Naval Research, DARPA, MathWorks, among others. His current research interests are in dynamic spectrum access networks and systems, wearables and implant communication and energy harvesting sensors.